

# Potentially Singular Behavior of the 3D Incompressible Navier-Stokes Equations

Thomas Y. Hou  
Applied and Comput, Math.  
Caltech

IPAM Workshop on Multiscale Modeling and Simulation  
in celebration of Russ Caflisch's 70th birthday

Supported by NSF and the Choi Family Gift Fund

April 26, 2024

# Motivation

The 3D Navier-Stokes equations describe the motion of viscous fluid:

$$\mathbf{u}_t + (\mathbf{u} \cdot \nabla)\mathbf{u} = -\nabla p + \nu \Delta \mathbf{u}, \quad \nabla \cdot \mathbf{u} = 0. \quad (1)$$

The special case of  $\nu = 0$  corresponds to the 3D Euler equations.

Define vorticity  $\boldsymbol{\omega} = \nabla \times \mathbf{u}$ , then  $\boldsymbol{\omega}$  is governed by

$$\boldsymbol{\omega}_t + (\mathbf{u} \cdot \nabla)\boldsymbol{\omega} = \nabla \mathbf{u} \cdot \boldsymbol{\omega} + \nu \Delta \boldsymbol{\omega}. \quad (2)$$

Note that  $\nabla \mathbf{u}$  is related to  $\boldsymbol{\omega}$  by a Riesz transform  $K$ :  $\nabla \mathbf{u} = K(\boldsymbol{\omega})$ , and the nonlocal vortex stretching term  $\nabla \mathbf{u} \cdot \boldsymbol{\omega}$  is formally of the order  $\boldsymbol{\omega}^2$ .

The cancellation between the transport and vortex stretching could lead to dynamic depletion of nonlinearity, thus prevent blowup.

## A brief review for 3D Euler equations

- **(Beale-Kato-Majda criterion, 1984)** A smooth solution develops a singularity at  $T$  if and only if  $\int_0^T \|\boldsymbol{\omega}(t)\|_\infty dt = \infty$ .
- **Geometry regularity of direction field of  $\boldsymbol{\omega}$ :** Constantin, Fefferman and Majda (1996). Let  $\boldsymbol{\omega} = |\boldsymbol{\omega}|\xi$ . The solution is smooth if  $\|\mathbf{u}(t)\|_{L^\infty(\Omega_t)}$  and  $\int_0^t \|\nabla\xi\|_{L^\infty(\Omega_\tau)}^2 d\tau$  are bounded.
- **Localized non-blow-up criteria,** Deng-Hou-Yu (2005). Let  $L_t$  be a vortex line segment around maximum vorticity. There is no blowup if  $\int_0^T \max_{L_t} |\mathbf{u}| dt < \infty$  and  $\int_{L_t} (|\kappa| + |\nabla \cdot \xi|) ds < \infty$ .
- Elgindi (2021): 3D Euler singularity with  $C^\alpha$  vorticity for axisymmetric Euler with no swirl ( $u^\theta \equiv 0$ ) and very small  $\alpha$ .

## A brief review for the NSE

- Global existence for small data (Leray, Ladyzhenskaya, Kato, etc). If  $\|\mathbf{u}_0\|_{L^p}$  ( $p \geq 3$ ) or  $\|\mathbf{u}_0\|_{L^2}\|\nabla\mathbf{u}_0\|_{L^2}$  is small, then the 3D Navier-Stokes equations have a globally smooth solution.
- Non-blowup criteria due to G. Prodi 59, J. Serrin 63. A weak solution  $\mathbf{u}$  of the 3D Navier-Stokes equations is smooth on  $[0, T] \times \mathbb{R}^3$  provided that  $\|\mathbf{u}\|_{L_t^q L_x^p([0, T] \times \mathbb{R}^3)} < \infty$  for some  $p, q$  satisfying  $\frac{3}{p} + \frac{2}{q} \leq 1$  with  $3 < p \leq \infty$  and  $2 \leq q < \infty$ .
- The critical case of  $p = 3, q = \infty$  was proved by L. Escauriaza, G. Seregin, and V. Sverak in 2003.
- **Partial regularity theory** (Caffarelli-Kohn-Nirenberg 82, F. Lin 98) For any suitable weak solution of the 3D Navier-Stokes equations on an open set in space-time, the one-dimensional Hausdorff measure of the associated singular set is zero.

## A brief review for the NSE – continued

- For the axisymmetric Navier-Stokes equations, Chen-Strain-Tsai-Yau (2007) and Koch-Nadirashvili-Seregin-Sverak (2007) proved that if  $|\mathbf{u}(\mathbf{x}, t)| \leq C|T - t|^{-1/2}$  and  $|\mathbf{u}(\mathbf{x}, t)| \leq \frac{C}{r}$  for  $r \geq r_0$ , then  $\mathbf{u}$  is regular up to  $T$ .
- T. Tao (2014) introduced an averaged NSE in the Fourier space:

$$u_t(x, t) + \tilde{B}(u, u) = \Delta_x u(x, t),$$

and showed that there exists a symmetric averaged bilinear operator  $\tilde{B}$  such that the solutions to the averaged NSE with a divergence-free initial data  $u_0$  blow up in finite time.

## Stabilizing effect of advection (Hou-Li, CPAM 2008)

The 3D axisymmetric Euler (Hou-Li, 2008) can be reformulated as

$$\begin{aligned}u_{1,t} + u^r u_{1,r} + u^z u_{1,z} &= 2u_1 \psi_{1,z}, \\ \omega_{1,t} + u^r \omega_{1,r} + u^z \omega_{1,z} &= (u_1^2)_z, \\ -\left[\partial_r^2 + \frac{3}{r} \partial_r + \partial_z^2\right] \psi_1 &= \omega_1, \quad u^r = -r\psi_{1,z}, \quad u^z = 2\psi_1 + r\psi_{1,r},\end{aligned}$$

for **smooth initial data**, where  $u_1 = u^\theta/r$ ,  $\omega_1 = \omega^\theta/r$ ,  $\psi_1 = \psi^\theta/r$ .

In [Hou-Li,2008], we studied the stabilizing effect of advection by considering a class of initial data  $u_0^\theta(r, z) = ru_0(z)$ ,  $\omega_0^\theta(r, z) = r\omega_0(z)$ .

We constructed a Lyapunov function  $(u_{1,z})^2 + \omega_1^2$  and showed that

$$((u_{1,z})^2 + \omega_1^2)_t + (u^r, u^z) \cdot \nabla_{r,z}((u_{1,z})^2 + \omega_1^2) = 0.$$

Advection cancels vortex stretching exactly, leading to global regularity.

# Review of numerical study of 3D Euler singularity

- On the numerical search for the Euler singularity:
  - Grauer and Sideris (1991): first numerical study of axisymmetric flows with swirl, blowup reported away from the axis;
  - Pumir and Siggia (1992): axisymmetric flows with swirl; blowup reported away from the axis;
  - Kerr (1993): **antiparallel vortex tubes; blowup reported;**
  - E and Shu (1994): 2D Boussinesq; **no blowup** observed;
  - Boratav and Pelz (1994): **viscous** simulations using Kida's high-symmetry initial condition; blowup reported;
  - Grauer et al. (1998): perturbed vortex tube; blowup reported;
  - Hou and Li (2006): **use Kerr's two anti-parallel vortex tube initial data; observed only double exponential growth of max vorticity.**
  - Charles Doering (UMich), Bartosz Protas (McMaster) used numerical optimization in space/time to search for potential blowup of Navier-Stokes, maximum vorticity grows less than a factor of 2.
  - Wang-Lai-Gomez-Serrano-Buckmaster (2022), used PINN to construct self-similar profiles of Hou-Luo blowup scenario.

# The 3D Euler blowup on the boundary, Luo-Hou 2014

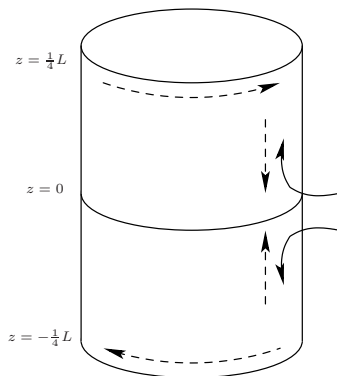


**Figure:** Vorticity kinematics of the 3D Euler singularity; solid: vortex lines; straight dashed lines: axial flow; curved dash lines: vortical circulation.



# Applying the Ideas: Computing the Line Fitting

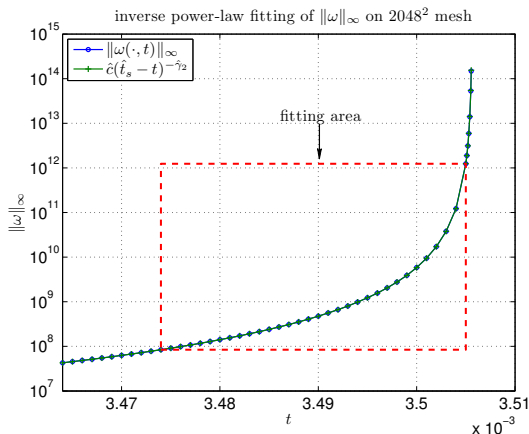


**Figure:** Maximum vorticity  $\|\omega\|_\infty$  and its inverse power-law fitting  $\hat{c}(T - t)^{-\hat{\gamma}_2}$  with  $\gamma_2 = 2.4579$ ,  $\omega \sim \frac{1}{(T-t)^{\gamma_2}} W\left(\frac{r-1, z}{(T-t)^{c_l}}\right)$  with  $c_l \approx 2.9215$ .

**Theorem 1** (Chen-Hou, 2022, 2023). There is a family of smooth initial data  $(\theta_0, \omega_0)$  with finite energy and boundary, such that the 2D Boussinesq and 3D Euler equations develop a stable and nearly self-similar finite time singularity.

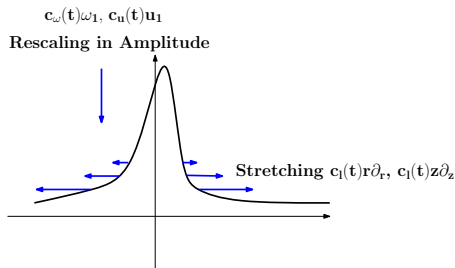
- Compared with the nonlinear Schrödinger equation or the Keller-Segel system, we do not have an analytic ground state,  $Q$ .
- Computer assistance is used to construct an approximate self-similar profile  $\bar{W}$  with a rigorously justified small residual  $O(10^{-7})$  in some singularly weighted  $L^\infty$  and  $C^{1/2}$  norm.
- We also need computer assistance to obtain sharp upper bounds for our stability constants involving singular integrals with singular kernels, singular weights, and the approximate profile.

# The Dynamic Rescaling Formulation

- Adding scaling terms to the 2D Boussinesq equation in  $\mathbb{R}_+^2$ :

$$\omega_\tau + (c_l(\tau)x + u) \cdot \nabla \omega = \theta_{x_1} + c_\omega(\tau)\omega, \quad \theta_\tau + (c_l(\tau)x + u) \cdot \nabla \theta = c_\theta(\tau)\theta.$$

- The  $c_l(\tau)x \cdot \nabla$  terms stretch the solutions in space.  
The  $c_\omega(\tau)\omega$  and  $c_\theta(\tau)\theta$  terms scale the solutions in amplitude.



- Using  $c_\theta(\tau) = c_l(\tau) - 2c_\omega(\tau)$ , the dynamic rescaling equations are equivalent to the original Boussinesq up to rescaling.

# The Equivalence Relation for Dynamic Rescaling

Let  $\theta(x, t)$ ,  $\omega(x, t)$  be solutions to the original 2D Boussinesq system,

$$C_\theta(\tau)\theta(C_l(\tau)x, t(\tau)), \quad C_\omega(\tau)\omega(C_l(\tau)x, t(\tau)),$$

are solutions to the dynamic rescaling equations, where

$$C_\theta(\tau) = e^{\int_0^\tau c_\theta(s)ds}, \quad C_\omega(\tau) = e^{\int_0^\tau c_\omega(s)ds}, \quad C_l(\tau) = e^{\int_0^\tau -c_l(s)ds}$$

and

$$t(\tau) = \int_0^\tau \exp\left(\int_0^s c_\omega(y)dy\right)ds.$$

**Remark 1:** if  $c_\omega(\tau) \rightarrow c_\omega < 0$ ,  $t(+\infty) = T < +\infty$  is the blowup time.

**Remark 2:** The dynamic rescaling formulation has been used by McLaughlin, Papanicolaou, Merle, Raphael, Martel, Zaag and others.

# A general approach to nonlinear stability

- Denote  $v = (\omega, \theta)^T$ , and write the dynamic rescaling equations as

$$\frac{d}{d\tau}v = F(v).$$

- Let  $\bar{v}$  be an approximate steady state of the dynamic rescaling equations:

$$\|F(\bar{v})\| = \varepsilon \ll 1.$$

- Decompose the solution as  $v = \bar{v} + \tilde{v}$ , then the equation for the perturbation  $\tilde{v}$  is

$$\frac{d}{d\tau}\tilde{v} = F(\bar{v} + \tilde{v}) = \underbrace{\nabla F(\bar{v})\tilde{v}}_{\text{Linear: } \mathcal{L}(\tilde{v})} + \underbrace{\tilde{v}^T \nabla^2 F(\bar{v})\tilde{v}}_{\text{Nonlinear: } N(\tilde{v})} + F(\bar{v}).$$

Note that  $F$  is bilinear in our problem.

# A general approach to nonlinear stability

- The perturbation solution  $\tilde{v}$  can be written as

$$\tilde{v}(\tau) = \int_0^\tau e^{(\tau-s)\mathcal{L}} (N(\tilde{v}) + F(\bar{v})) ds.$$

- Assume that the linearized operator around the approximate steady state enjoys certain stability with a suitable norm:

$$\|e^{\tau\mathcal{L}}\| \leq e^{-\lambda\tau}, \quad \lambda > 0,$$

and assume that the nonlinear term can be bounded as

$$\|N(\tilde{v})\| \leq C\|\tilde{v}\|^2.$$

Then we have

$$\|\tilde{v}(\tau)\| \leq \int_0^\tau e^{-\lambda(\tau-s)} (C\|\tilde{v}(s)\|^2 + \varepsilon) ds.$$

# A general approach to nonlinear stability

- If  $4\epsilon C < \lambda^2$ , there exists some  $\delta > 0$  such that

$$\frac{C\delta^2}{\lambda} + \frac{\epsilon}{\lambda} \leq \delta.$$

- Bootstrapping: suppose that  $\|\tilde{v}(s)\| \leq \delta$  for all  $s \in [0, \tau)$ , then

$$\|\tilde{v}(\tau)\| \leq \int_0^\tau e^{-\lambda(\tau-s)} (C\delta^2 + \epsilon) ds < \frac{C\delta^2}{\lambda} + \frac{\epsilon}{\lambda} \leq \delta,$$

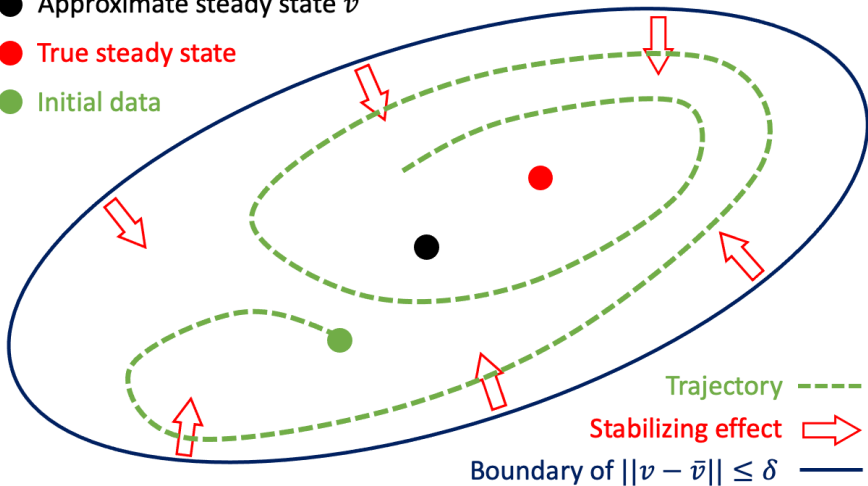
which means that  $\|\tilde{v}(\tau)\| \leq \delta$  for all time given  $\|\tilde{v}(0)\| \leq \delta$ .

- The dynamic rescaling solution  $v(\tau) = \bar{v} + \tilde{v}(\tau)$  will not escape a norm ball of radius  $\delta$  around the approximate steady state  $\bar{v}$ .
- We turn the problem of proving **finite time singularity** into the problem of **long time stability of an approximate blowup profile**.

● Approximate steady state  $\bar{v}$

● True steady state

● Initial data





- We study potential singularity of the 3D axisymmetric Euler and potentially singular behavior of the 3D Navier–Stokes equations:

$$\mathbf{u}_t + \mathbf{u} \cdot \nabla \mathbf{u} = -\nabla p + \nu \Delta \mathbf{u}, \quad \nabla \cdot \mathbf{u} = 0. \quad (3)$$

- Introduce a change of variables:  $u_1 = u^\theta/r$ ,  $\omega_1 = \omega^\theta/r$ , and  $\psi_1 = \psi^\theta/r$ . The equations (3) can be rewritten in an equivalent form:

$$\begin{cases} u_{1,t} + u^r u_{1,r} + u^z u_{1,z} = 2u_1 \psi_{1,z} + \nu \Delta u_1, \\ \omega_{1,t} + u^r \omega_{1,r} + u^z \omega_{1,z} = 2u_1 \omega_{1,z} + \nu \Delta \omega_1, \\ -\left(\partial_r^2 + \frac{3}{r} \partial_r + \partial_z^2\right) \psi_1 = \omega_1, \\ u^r = -r \psi_{1,z}, \quad u^z = 2\psi_1 + r \psi_{1,r}. \end{cases} \quad (4)$$

## The axisymmetric formulation

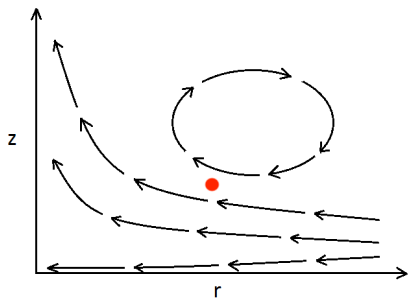
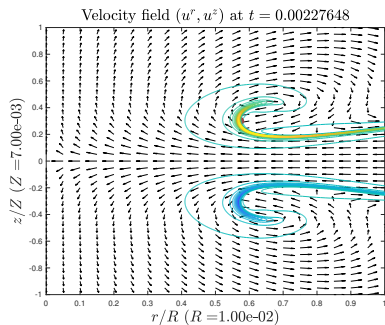
- Our smooth initial condition has a very simple form:

$$u^\theta(0, r, z) = \frac{12000r(1 - r^2)^{18} \sin(2\pi z)}{1 + 12.5(\sin(\pi z))^2}, \quad \omega^\theta(0, r, z) = 0. \quad (5)$$

An important feature of this initial data is that it produces nearly self-similar scaling properties compatible with those of the NSE.

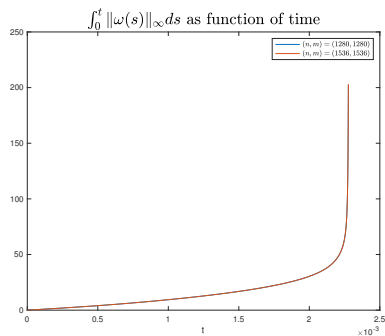
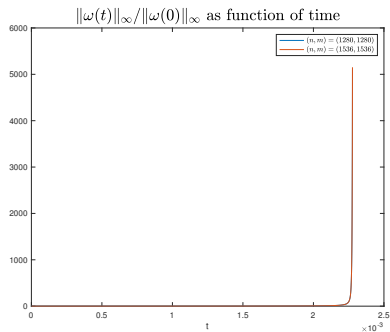
- Our new initial condition shares several features with the two-scale traveling wave singularity using variable diffusion coefficients  $\nu(r, z) = O(r^2 + z^2)$  with De Huang (Physica D, 2022, MMS, 2023).
- However, the two-scale travel wave solution does not survive viscous regularization since the small scale  $Z(t) \sim (T - t)$  and  $R(t) \sim \sqrt{T - t}$ . The maximum vorticity with  $\nu = 10^{-5}$  increases less than a factor of 2. The solution also suffers from tail instability.

## Dipole structure of $\omega^\theta$



- The odd symmetry of  $\omega^\theta$  (in  $z$ ) induces a hyperbolic flow structure and a vortex dipole, which generate a negative radial velocity field and push the solution near  $z = 0$  towards to symmetry axis  $r = 0$ .

## Rapid growth of maximum vorticity



- Left plot: the amplification of maximum vorticity relative to its initial maximum vorticity,  $\|\omega(t)\|_{L^\infty} / \|\omega(0)\|_{L^\infty}$  as a function of time. Right plot: the time integral of maximum vorticity,  $\int_0^t \|\omega(s)\|_{L^\infty} ds$  as a function of time.

## A tornado singularity, a global view of 3D streamlines

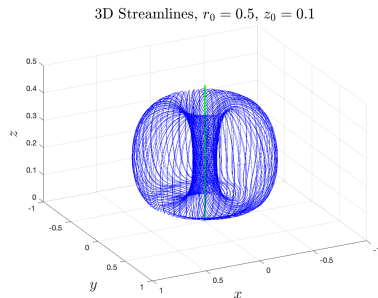
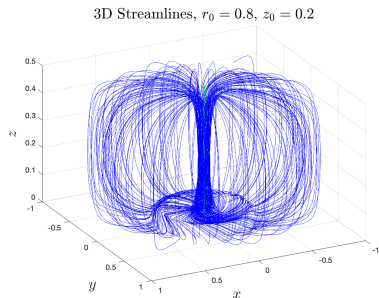


**Figure:** The 3D streamlines of at time  $t = 0.00227648$  with different initial points. The 3D velocity field  $(u^r, u^z, u^\theta)$  is a tornado solution with a quiet wind eye.

## A tornado singularity, a local view of 3D streamlines

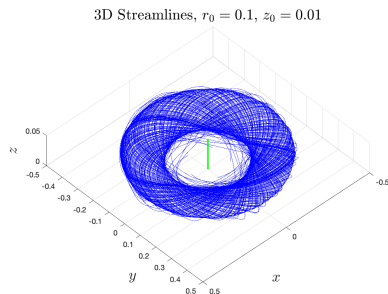
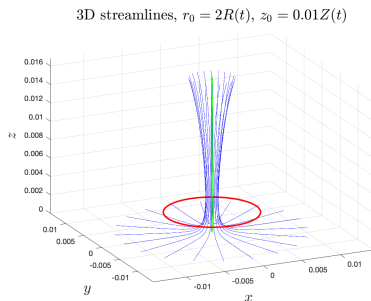
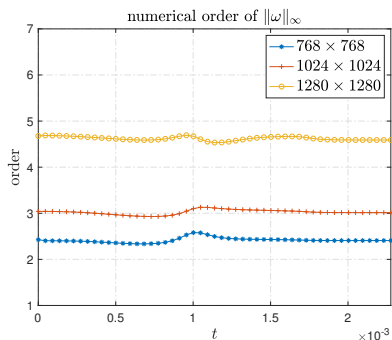
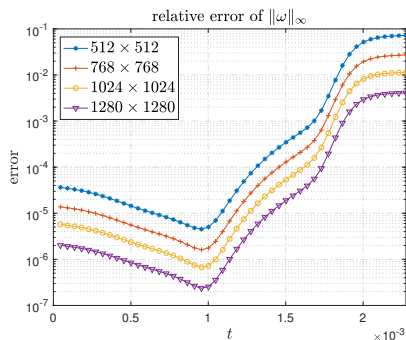


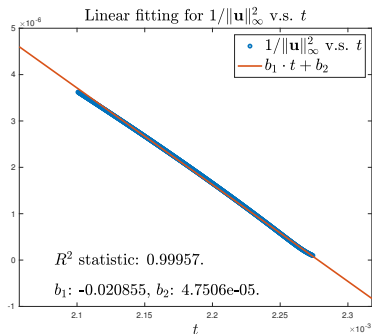
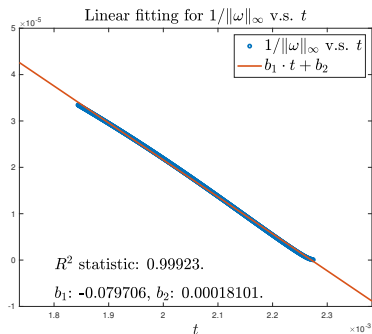
**Figure:** The 3D streamlines of at time  $t = 0.00227648$  with different initial points. The 3D velocity field  $(u^r, u^z, u^\theta)$  is a tornado solution with a quiet wind eye.

## Convergence study



- Relative error and numerical order of  $\|\omega(t)\|_{L^\infty}$ . The last time instant shown in the figure is  $t = 0.00227648$ .

## Linear fitting of maximum vorticity and velocity



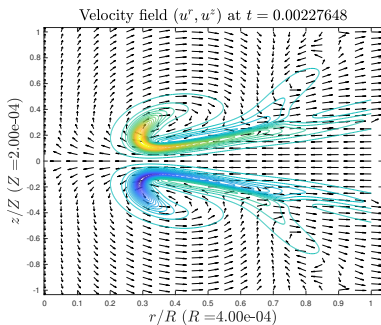
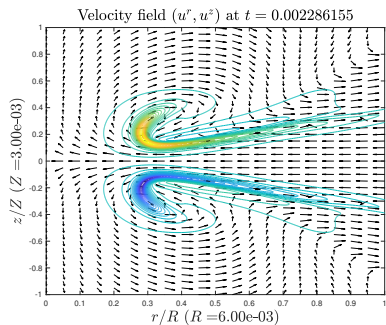
- The linear regression of (a)  $\|\omega(t)\|_{L^\infty}^{-1}$  vs  $t$ , (b)  $\|\mathbf{u}(t)\|_{L^\infty}^{-2}$  vs  $t$ . This implies that  $\|\omega(t)\|_{L^\infty} \sim \frac{1}{T-t}$  and  $\|\mathbf{u}(t)\|_{L^\infty} \sim \frac{1}{(T-t)^{1/2}}$ . This suggests that the vorticity blows up like  $\omega \sim \frac{1}{(T-t)} \Omega\left(\frac{(r-R(t), z-Z(t))}{(T-t)^{1/2}}, t\right)$ .



## The potentially singular behavior of 3D NSE

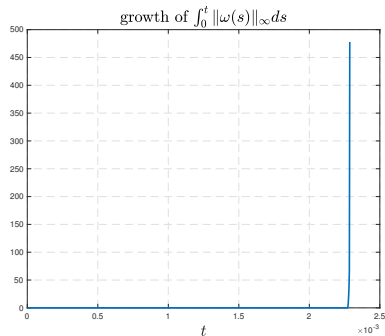
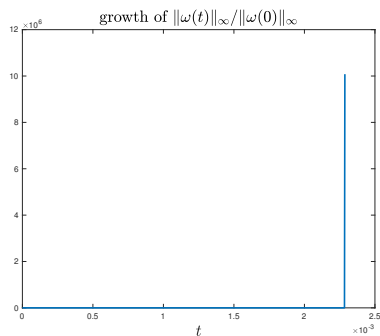
- Given that the scaling properties of the 3D Euler equations are compatible with those of the 3D Navier-Stokes equations, it is natural to investigate whether the Navier-Stokes equations with the same initial condition would develop a singularity.
- It turns out that the choice of the viscosity is important in producing a nearly singular behavior of the NSE.
- We will first use  $\nu = 5 \cdot 10^{-4}$  from  $t = 0$  to  $t_1 = 0.00227375$ , then increase  $\nu$  to  $5 \cdot 10^{-3}$  for  $t \geq t_1$ .
- This relatively large viscosity enhances the nonlinear alignment of vortex stretching, producing a relative long stable phase of strong nonlinear alignment and a nearly singular solution at the origin.

## Dipole structure of $\omega_1$



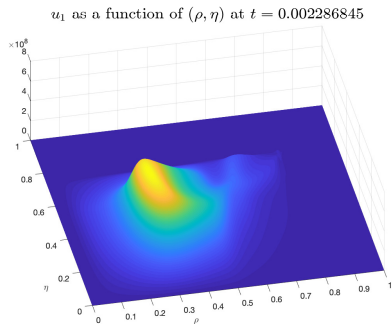
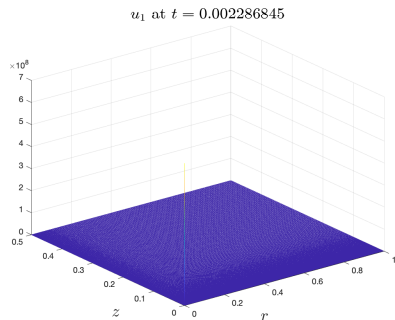
- The odd symmetry of  $\omega_1$  (in  $z$ ) induces a flow structure that has the desirable property of pushing the solution near  $z = 0$  towards to symmetry axis  $r = 0$ .

## Rapid growth of maximum vorticity



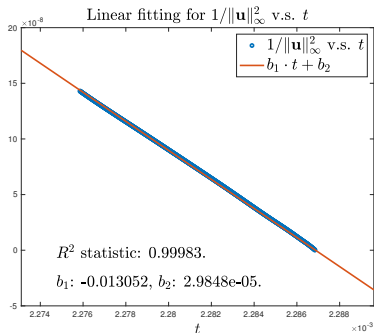
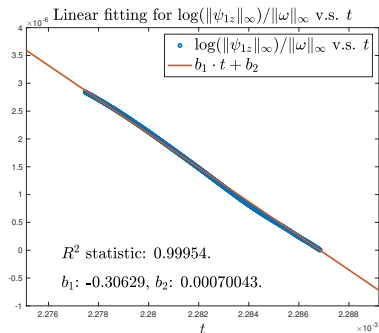
- Left plot: the amplification of maximum vorticity relative to its initial maximum vorticity,  $\|\omega(t)\|_{L^\infty}/\|\omega(0)\|_{L^\infty}$  as a function of time, growing by a factor of  $10^7$ . Right plot: the time integral of maximum vorticity,  $\int_0^t \|\omega(s)\|_{L^\infty} ds$  as a function of time.

## Resolution study



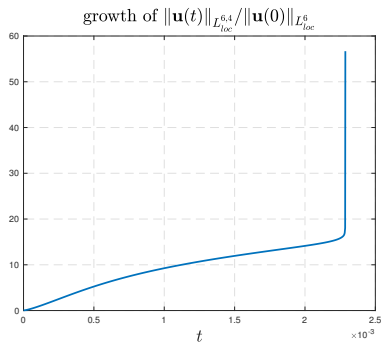
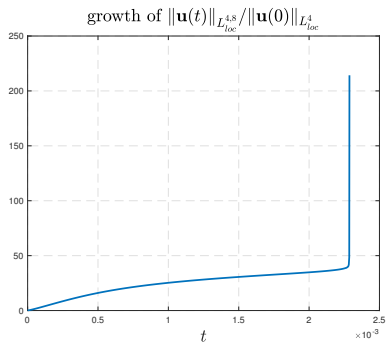
- (a):  $u_1$  in the whole physical coordinates  $r, z$ .
- (b):  $u_1$  in the transformed coordinates  $(\rho, \eta)$ .

## Linear fitting of maximum vorticity and velocity



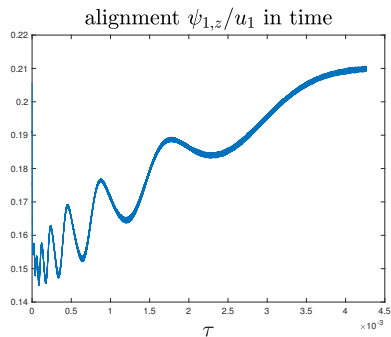
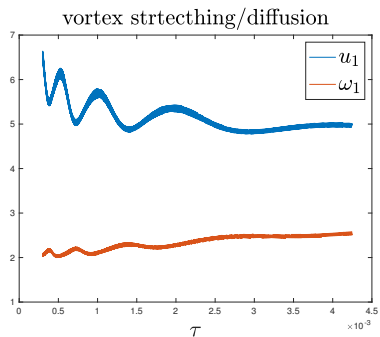
- The linear regression of (a)  $\log(\|\psi_{1z}(t)\|_{L^\infty})\|\omega(t)\|_{L^\infty}^{-1}$  vs  $t$ , (b)  $\|\mathbf{u}(t)\|_{L^\infty}^{-2}$  vs  $t$ . This implies that  $\|\omega(t)\|_{L^\infty} \sim \frac{|\log(T-t)|}{T-t}$  and  $\|\mathbf{u}(t)\|_{L^\infty} \sim \frac{1}{(T-t)^{1/2}}$ . We observe that  $Z(t) \sim (T-t)^{1/2}$  with a logarithmic correction.

## Further evidence—continued



Left subplot:  $\|\mathbf{u}\|_{L_{loc}^{4,8}} = (\int_0^t \|\mathbf{u}(s)\|_{L_{loc}^4}^8 ds)^{1/8}$ . Right subplot:  $\|\mathbf{u}\|_{L_{loc}^{6,4}}$ .

## Nearly self-similar scaling properties – continued



Left plot: Vortex stretching/diffusion. Right plot: Alignment between  $\psi_{1,z}$  and  $u_1$  at  $(R(\tau), Z(\tau))$ . We solve  $(u_1)_t + \mathbf{u} \cdot \nabla u_1 = 2\psi_{1,z}u_1 + \nu\Delta u_1$  and  $(\omega_1)_t + \mathbf{u} \cdot \nabla \omega_1 = 2u_1u_{1,z} + \nu\Delta \omega_1$ .

We consider a generalized axisymmetric Navier–Stokes equation in  $n$  dimensions with  $n = 1 + 2R(t)/Z(t)$  and  $(R(t), Z(t)) = \arg \max(u_1)$ :

$$\begin{aligned} u_{1,t} + u^r u_{1,r} + u^z u_{1,z} &= 2\psi_{1,z} u_1 + \nu \Delta_{n+2} u_1 \\ \omega_{1,t} + u^r \omega_{1,r} + u^z \omega_{1,z} &= (u_1^2)_z - (n-3)\psi_{1,z} \omega_1 + \nu \Delta_{n+2} \omega_1 \\ -\Delta_{n+2} \psi_1 &= \omega_1, \quad \Delta_{n+2} = \partial_r^2 + \frac{n}{r} \partial_r + \partial_z^2, \end{aligned}$$

where  $u^r = -(r^{n-2} \psi^\theta)_z / r^{n-2}$ ,  $u^z = (r^{n-2} \psi^\theta)_r / r^{n-2}$ . It satisfies a generalized incompressibility condition  $(r^{n-2} u^r)_r + (r^{n-2} u^z)_z = 0$ , the conservation of total circulation  $\Gamma = r u^\theta$ , and the energy conservation

$$\frac{d}{dt} \int |\mathbf{u}|^2 r^{n-2} dr dz = -\nu \int |\nabla \mathbf{u}|^2 r^{n-2} dr dz.$$



We also consider a generalized axisymmetric Boussinesq system in  $n$  dimensions by treating  $\Gamma$  as density and removing  $(n - 3)\psi_{1,z}\omega_1$ :

$$\Gamma_t + u^r \Gamma_r + u^z \Gamma_z = \nu_1 \left( \Gamma_{rr} + \frac{(n-4)}{r} \Gamma_r + \frac{(6-2n)}{r^2} \Gamma + \Gamma_{zz} \right), \quad (6a)$$

$$\omega_{1,t} + u^r \omega_{1,r} + u^z \omega_{1,z} = \left( \frac{\Gamma^2}{r^4} \right)_z + \nu_2 \left( \omega_{1,rr} + \frac{n}{r} \omega_{1,r} + \omega_{1,zz} \right), \quad (6b)$$

$$- \left( \partial_r^2 + \frac{n}{r} \partial_r + \partial_z^2 \right) \psi_1 = \omega_1, \quad (6c)$$

where  $u^r = -(r^{m-2}\psi^\theta)_z/r^{m-2}$ ,  $u^z = (r^{m-2}\psi^\theta)_r/r^{m-2}$ ,  $n = 2m - 3$ ,  $m = 1 + 2R(t)/Z(t)$ . It satisfies the incompressibility condition  $(r^{m-2}u^r)_r + (r^{m-2}u^z)_z = 0$ , the conservation of total circulation. If  $n < 7$ , the energy  $\int (|u^\theta|^2 + \frac{(7-n)}{4} (|u^r|^2 + |u^z|^2) r^{n-2} dr dz)$  is conserved.

In the case of  $\nu_1 = \nu_2 = \nu_0 \|u_1\|_\infty Z(t)^2$ , we have  $\nu_i C_\psi / C_{l_z} = \nu_0$ , and  $\tilde{\psi}_1, \tilde{u}_1, \tilde{\omega}_1$  satisfy the following dynamic rescaling equations

$$\begin{aligned} \tilde{\Gamma}_\tau + c_{lr} \xi \tilde{\Gamma}_\xi + c_{lz} \eta \tilde{\Gamma}_\eta + \tilde{\mathbf{u}} \cdot \nabla_{(\xi, \eta)} \tilde{\Gamma} &= c_\Gamma \tilde{\Gamma} + \nu_0 \tilde{\Delta} \tilde{\Gamma}, \\ \tilde{\omega}_{1, \tau} + c_{lr} \xi \tilde{\omega}_{1, \xi} + c_{lz} \eta \tilde{\omega}_{1, \eta} + \tilde{\mathbf{u}} \cdot \nabla_{(\xi, \eta)} \tilde{\omega}_1 &= c_\omega \tilde{\omega}_1 + \left( \frac{\tilde{\Gamma}^2}{\xi^4} \right)_\eta + \nu_0 \Delta \tilde{\omega}, \\ -\Delta \tilde{\psi}_1 = \tilde{\omega}_1, \quad \Delta &= - \left( \delta^2 \partial_\xi^2 + \delta^2 \frac{n}{\xi} \partial_\xi + \partial_\eta^2 \right), \end{aligned}$$

where  $\delta = C_{l_z}(\tau) / C_{l_r}(\tau)$  and  $(c_{l_z}, c_{l_r}, c_\psi, c_u, c_\omega)$  satisfy the relationship

$$c_\psi = c_u + c_{l_z}, \quad c_\omega = c_u - c_{l_z}, \quad c_\Gamma = c_u + 2c_{l_r} = 2(c_{l_r} - c_{l_z}).$$

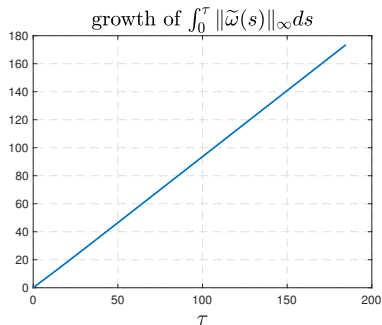
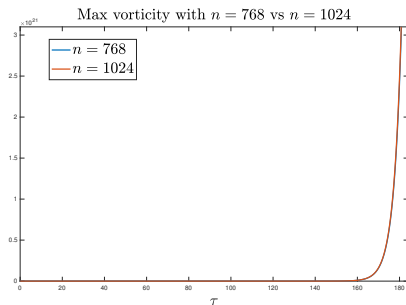
Thus, the self-similar profile satisfies the generalized Navier–Stokes equations with constant viscosity  $\nu_0$ .

We take  $\nu = \nu_0 \|u_1(t)\|_\infty Z(t)^2$  where  $(R(t), Z(t))$  is where  $u_1$  achieves its maximum and choose  $n = 1 + 2R(t)/Z(t)$  so that  $u^r$  and  $u^z$  scale like  $(R(t)/Z(t))\psi_1$ . We obtain a self-similar blowup with  $n \approx 3.188$ :

$$\begin{aligned} \psi_1(t, r, z) &= \frac{\lambda(t)}{(T-t)^{1/2}} \Psi_1 \left( \tau, \frac{r}{\lambda(t)\sqrt{(T-t)}}, \frac{z}{\lambda(t)\sqrt{(T-t)}} \right), \\ u_1(t, r, z) &= \frac{1}{(T-t)} V_1 \left( \tau, \frac{r}{\lambda(t)\sqrt{(T-t)}}, \frac{z}{\lambda(t)\sqrt{(T-t)}} \right), \\ \omega_1(t, r, z) &= \frac{1}{\lambda(t)(T-t)^{3/2}} \Omega_1 \left( \tau, \frac{r}{\lambda(t)\sqrt{(T-t)}}, \frac{z}{\lambda(t)\sqrt{(T-t)}} \right), \end{aligned}$$

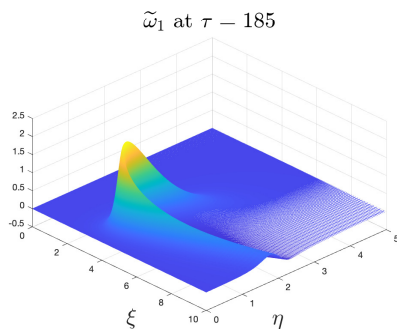
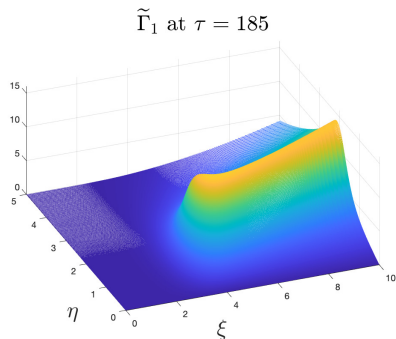
where  $\lambda(t) = (T-t)^{0.023}$  and  $R(\tau)/Z(\tau) \rightarrow 1.09$  as  $\tau \rightarrow \infty$ .

# Self-similar blowup of the generalized Navier–Stokes with decaying viscosity



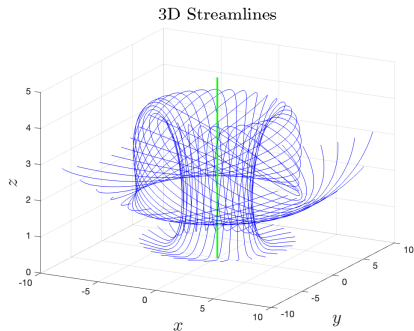
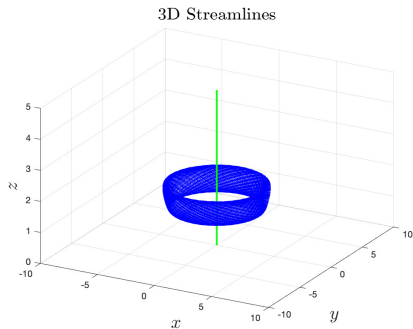
Left plot: Growth of  $\|\omega(\tau)\|_{L^\infty}$  in  $\tau$  using  $768 \times 768$  vs  $1024 \times 1024$ .  
Right plot: Growth of  $\int_0^\tau \|\tilde{\omega}(s)\|_{L^\infty} ds$  in  $\tau$ .

# Nearly self-similar blowup of generalized Navier-Stokes with vanishing viscosity



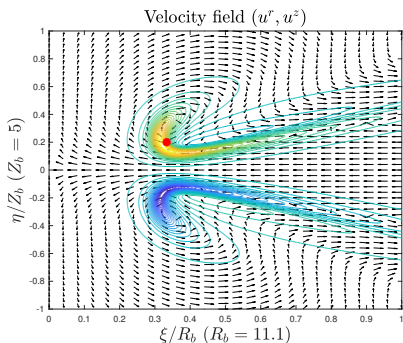
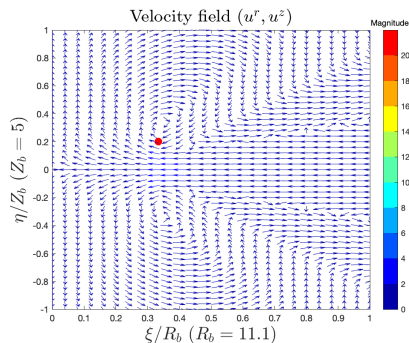
Left subplot: 3D plot of  $\tilde{\Gamma}$  at  $\tau = 185$ . Right subplot: 3D plot of  $\tilde{\omega}_1$  at  $\tau = 185$ .

## Nearly self-similar blowup of generalized Navier-Stokes with decaying viscosity



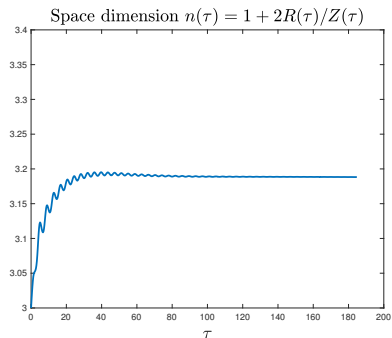
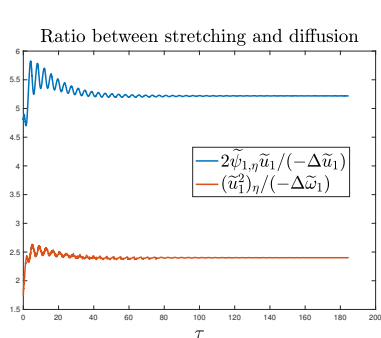
Left subplot: Streamlines at  $\tau = 185$  with  $(r_0, z_0) = (4, 2)$ . Right subplot: Streamlines at  $\tau = 185$  with  $(r_0, z_0) = (6, 0.5)$ .

# Nearly self-similar blowup of generalized Navier-Stokes with decaying viscosity



The dipole structure of  $\omega_1$  and the induced local velocity field at  $\tau = 185$ . Left plot: the velocity vector. Right plot: the velocity vector with the  $\omega_1$  contour as background.

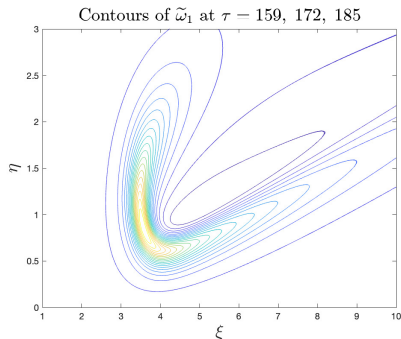
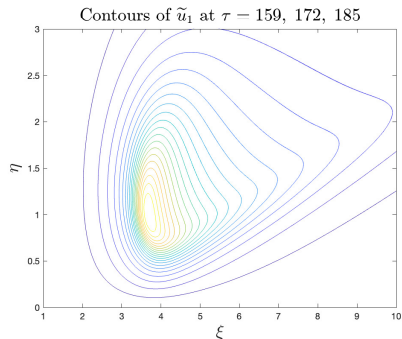
## Nearly self-similar blowup of generalized Navier-Stokes with decaying viscosity



Left plot: The ratio between vortex stretching and diffusion for  $\tilde{u}_1$  at  $(R, Z)$  and for  $\tilde{\omega}_1$  at  $(R_\omega, Z_\omega)$ .  $u_{1,t} + \mathbf{u} \cdot \nabla u_1 = 2\psi_{1,z}u_1 + \nu(t)\Delta u_1$ ,  $\omega_{1,t} + \mathbf{u} \cdot \nabla \omega_1 = (u_1^2)_z - (n-3)\psi_{1,z}\omega_1 + \nu(t)\Delta \omega_1$ . Right plot: The dimension  $n(\tau) = 1 + 2R(\tau)/Z(\tau)$  with  $n(185) = 3.188$ .



## Nearly self-similar blowup of generalized Navier-Stokes with vdecaying viscosity



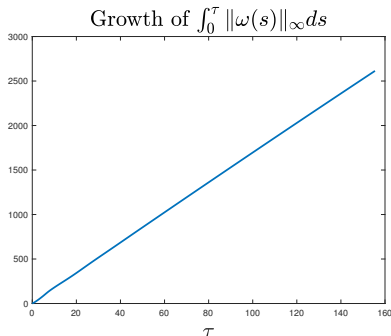
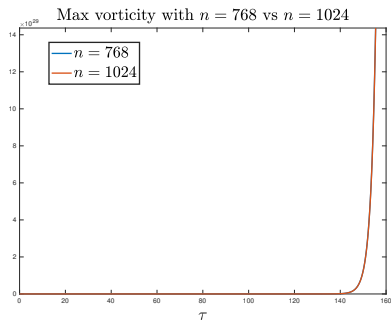
Left plot: Contours of  $\tilde{u}_1$  at  $\tau = 159, 172, 185$  during which  $\|\omega\|_\infty$  has increased by 1029. Right plot: Contours of  $\tilde{\omega}_1$  at  $\tau = 159, 172, 185$ .

By taking  $\nu_1 = 6 \times 10^{-4}$ ,  $\nu_2 = 10\nu_1$ , we obtain a new blowup scenario:

$$\begin{aligned}\psi_1(t, r, z) &= \frac{\lambda(t)}{(T-t)^{1/2}} \Psi_1 \left( \tau, \frac{r}{\lambda(t)\sqrt{(T-t)}}, \frac{z}{\lambda(t)\sqrt{(T-t)}} \right), \\ u_1(t, r, z) &= \frac{1}{(T-t)} V_1 \left( \tau, \frac{r}{\lambda(t)\sqrt{(T-t)}}, \frac{z}{\lambda(t)\sqrt{(T-t)}} \right), \\ \omega_1(t, r, z) &= \frac{1}{\lambda(t)(T-t)^{3/2}} \Omega_1 \left( \tau, \frac{r}{\lambda(t)\sqrt{(T-t)}}, \frac{z}{\lambda(t)\sqrt{(T-t)}} \right),\end{aligned}$$

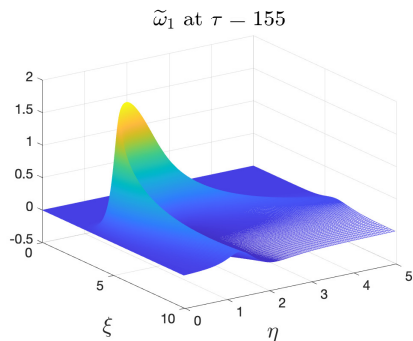
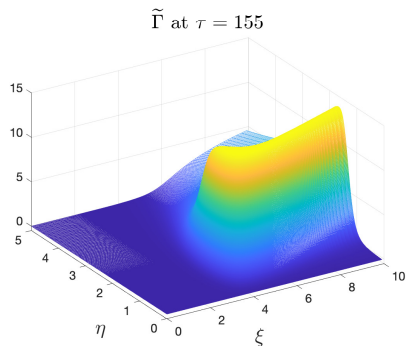
where  $\lambda(t) = (1 + \epsilon |\log(T-t)|)^{-1/2}$ . We vary the dimension continuously by modifying  $u^r = -r\psi_{1,z}$  and  $u^z = (m-1)\psi_1 + r\psi_{1,r}$  with  $(m-1) = 2R(t)/Z(t)$ .  $u^r$  and  $u^z$  now scale like  $(R(t)/Z(t))\psi_1$ .

## Generalized Boussinesq system with 2 constant viscosity coefficients



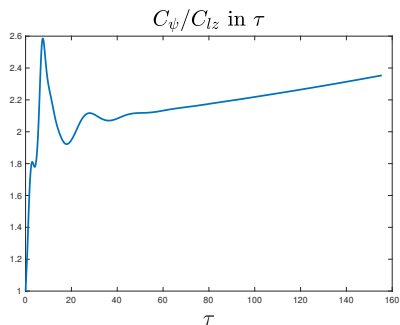
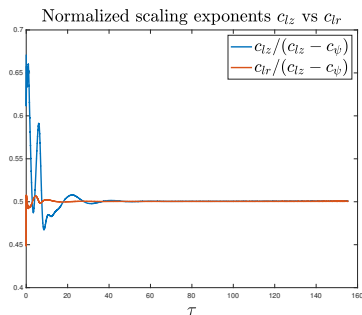
Left plot: Growth of  $\|\omega(\tau)\|_{L^\infty}$  in  $\tau$  using  $768 \times 768$  vs  $1024 \times 1024$ .  
Right plot: Growth of  $\int_0^\tau \|\tilde{\omega}(s)\|_{L^\infty} ds$  in  $\tau$ .

## Generalized Boussinesq system with 2 constant viscosity coefficients



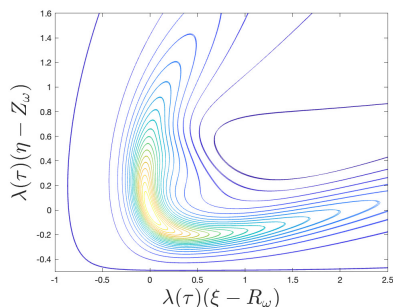
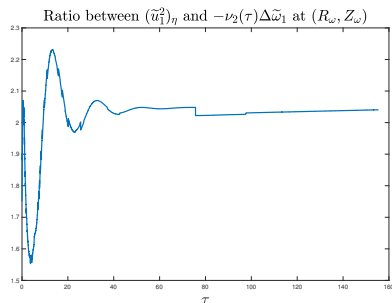
Left subplot: 3D plot of  $\tilde{\Gamma}$  at  $\tau = 155$ . Right subplot: 3D plot of  $\tilde{\omega}_1$  at  $\tau = 155$ .

## Generalized Boussinesq system with 2 constant viscosity coefficients



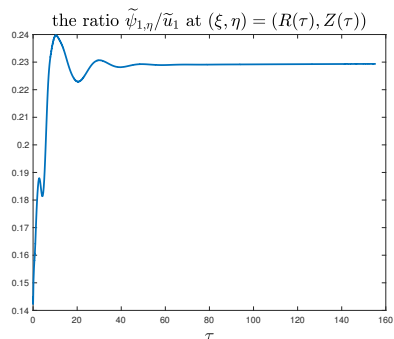
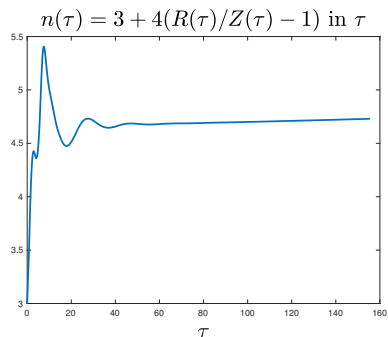
Left plot: The normalized scaling exponent  $c_{lz}$  for  $Z(t) \sim (T - t)^{c_{lz}}$  and  $c_{lr}$  for  $R(t) \sim (T - t)^{c_{lr}}$  in  $\tau$ . Right plot:  $C_\psi(\tau)/C_{lz}(\tau) = 1/\lambda(\tau)^2$ . The almost linear growth in  $\tau$  implies that  $c_{lz}$  and  $c_{lr}$  converge to  $1/2$  and  $\lambda = (1 + \epsilon\tau)^{-1/2} = (1 + \epsilon|\log(T - t)|)^{-1/2}$ .

## Generalized Boussinesq system with 2 constant viscosity coefficients



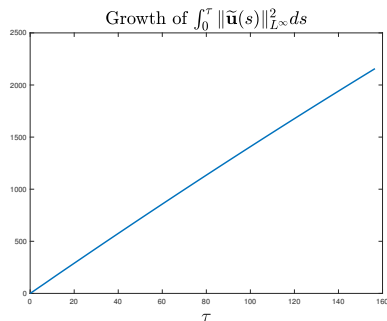
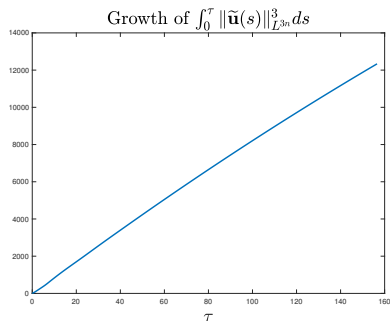
Left plot: The ratio between vortex stretching and diffusion for  $\tilde{\omega}_1$ .  
Right plot: Contours of  $\tilde{\omega}_1$  with respect to  $((\xi - R_\omega)\lambda(\tau), (\eta - Z_\omega)\lambda(\tau))$  at  $\tau = 139, 147, 155$  during which  $\|\boldsymbol{\omega}\|_\infty$  has increased by 1554.

## Generalized Boussinesq system with 2 constant viscosity coefficients



Left plot: The dimension  $n(\tau) = 3 + 4(R(\tau)/Z(\tau) - 1)$  with  $n(155) = 4.73$ . Right plot: The ratio  $\tilde{\psi}_{1,\eta}/\tilde{u}_1$  at  $(R(\tau), Z(\tau))$ .

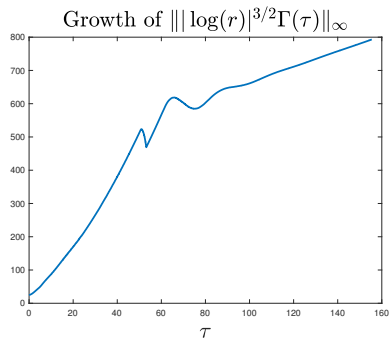
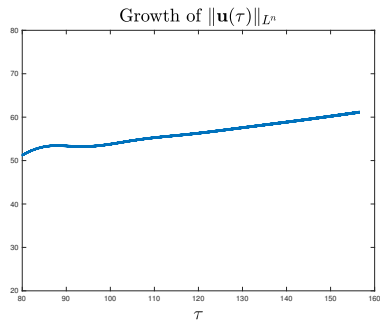
## Generalized Boussinesq system with 2 constant viscosity coefficients



Serrin-Prodi criteria  $n/p + 2/q \leq 1$ . Left plot:  $\int_0^\tau \|\tilde{\mathbf{u}}(s)\|_{L^{3n}}^3 ds$  in  $\tau$ . The linear fitting implies  $\|\mathbf{u}(\tau)\|_{L^{3n,3}} \sim O(\tau^{1/3})$ . Right plot:  $\int_0^\tau \|\tilde{\mathbf{u}}(s)\|_{L^\infty}^2 ds$ . The linear fitting implies  $\|\mathbf{u}(\tau)\|_{L^\infty} \sim O(\tau^{1/2})$ .

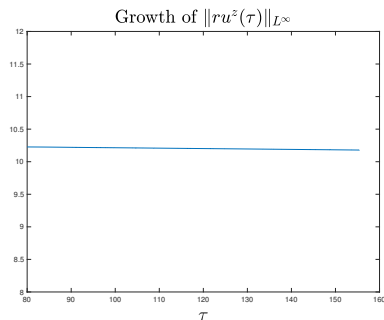
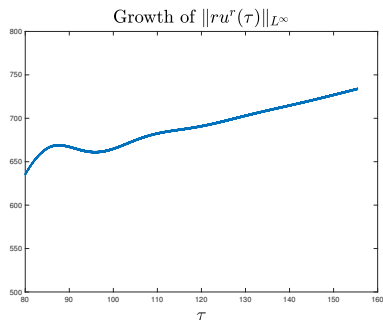


## Generalized Boussinesq system with 2 constant viscosity coefficients



Left plot: The end point case with  $p = n, q = \infty$ :  $\|\mathbf{u}\|_{L^n}$ . Right plot:  $\| |\log(r)|^{3/2} \Gamma(\tau, r, z) \|_{L^\infty}$  in  $\tau$ . Dongyi Wei (2017) showed that the axisymmetric NSE cannot blowup if  $\| |\log(r)|^{3/2} \Gamma(\tau, r, z) \|_{r \leq r_0} \leq 1$ .

## Solving Navier-Stokes using new initial data– continued



Left plot: The dynamic growth of  $\|ru^r\|_{L^\infty}$  as a function of  $\tau$ . Right plot: The dynamic growth of  $\|ru^z\|_{L^\infty}$  as a function of  $\tau$ . This violates the non-blowup criteria by Sverak (2007) et al and Yau et al (2007).

# Summary

- We presented a new class of initial data that lead to a potentially singular solution of the axisymmetric Euler at the origin.
- An important feature of this potentially singular solution is that the scaling properties are compatible with those of the NSE.
- We demonstrated the potentially singular behavior of 3D Navier-Stokes with maximum vorticity increased by a factor of  $10^7$ .
- We demonstrated a generalized Navier–Stokes and a generalized Boussinesq system with constant viscosity develops a nearly self-similar blowup with maximum vorticity increased by  $10^{30}$ .
- We used a novel two-scale dynamic rescaling formulation and a conservative formulation to capture the logarithmic correction.

Happy Birthday, Russ!

## References.

- J. Chen and T. Y. Hou, *Stable nearly self-similar blowup of the 2D Boussinesq and 3D Euler equations with smooth data. Part I. Analysis, arXiv:2210.07191v2 [math.AP], Part II: Rigorous Numerics, accepted by MMS. arXiv:2305.05660 [math.AP]*.
- T, Y. Hou, The Nearly Singular Behavior of the 3D Navier-Stokes Equations, published online on 9/7/2022, DOI: <https://doi.org/10.1007/s10208-022-09578-4>.
- T, Y. Hou and D. Huang, *A potential two-scale traveling wave singularity for 3D incompressible Euler equations, Physica D, Vol 435, 133257, 2022.*
- T. Y. Hou, Nearly self-similar blowup of generalized axisymmetric Navier–Stokes and Boussinesq equations, arXiv:2405.10916 [math.AP], 2024.